Role of aerosol size distribution and source location in a three- dimensional simulation of a Saharan dust episode tested against satellite-derived optical thickness

Michael Schulz, Yves Balkanski, Walter Guelle, François Dulac

JOURNAL OF GEOPHYSICAL RESEARCH, VOL. 103, NO. D9, PAGES 10,579–10,592, MAY 20, 1998

Role of aerosol size distribution and source location in a three-dimensional simulation of a Saharan dust episode tested against satellite-derived optical thickness

Michael Schulz[1]

Centre des Faibles Radioactivités, CNRS-CEA, Gif-sur-Yvette, France

Yves J. Balkanski and Walter Guelle

Laboratoire de Modélisation du Climat et de l'Environnement, CEA, CE Saclay, France

Francois Dulac

Centre des Faibles Radioactivités, CNRS-CEA, Gif-sur-Yvette, France

Abstract. An off-line global three-dimensional tracer model based on analyzed wind fields was augmented to simulate the atmospheric transport of mineral dust. The model describes the evolution of the aerosol size distribution and hence allows to compute aerosol number and mass concentrations. In this study we describe the parameterization of the sedimentation process and include a preliminary source formulation but exclude wet deposition. Validation of the model is done during a 16-day period in June-July 1988 with very scarce precipitation. It is based on a comparison of every model grid box with daily satellite-derived optical thickness observations of Saharan dust plumes over the North Atlantic and the Mediterranean. The model reproduces accurately the daily position of the dust plumes over the ocean, with the exception of Atlantic regions remote from the African coast. By systematic analysis of transport and aerosol components we show that the largest uncertainty in reproducing the position of the dust clouds is the correct localization of the source regions. The model simulation is also very sensitive to the inclusion of convection and to an accurate treatment of the sedimentation process. Only the combination of source activation, rapid transport of dust to higher altitudes by convective updraft and long-range transport allows the simulation of the dust plumes position. This study shows that a mineral dust transport model is only constrained if both the source strength and the aerosol size distribution are known. The satellite observation of optical thickness over the Mediterranean and assumptions about the size distribution indicate that the dust emission flux was of the order of 17×10^6 t for the 16-day period under investigation. The simulations suggest that a major aerosol mode initially around 2 5 μm with a standard deviation of 2.0 plays the dominant role in long-range transport of mineral dust.

1. Introduction

A renewed interest in dust comes from the role played by the large quantity of mineral aerosols in the Earth radiative budget [*Houghton et al.*, 1994] which might be significantly disturbed by anthropogenic activities [*Andreae*, 1996; *Tegen et al.*, 1996]. Furthermore, the surface of desert dust particles provides a substrate for heterogeneous chemistry [*Dentener et al*, 1996]. Mineral aerosols transported at far distances also play a role in providing micronutrients to remote ecosystems and may stimulate marine and terrestrial productivity [*Martin and Fitzwater*, 1988; *Swap et al.*, 1992; *Martin et al.*, 1994]. In order to apprehend these effects on a global and possibly historical scale, one has to show that the present atmospheric dust transport can be described accurately in a model. Such a description of the dust transport has been up to now a challenge,
because of the difficulty in representing the following processes the source potential of certain regions depending on their specific soil type and vegetation resulting in localized dust storms of brief duration; the long-range transport over thousands of kilometers and the removal and transformation processes that affect the aerosol size distribution.

With regard to experimental access to the problem, satellite observations provide an invaluable way to assess the extension and frequency of appearance of dust clouds over the oceans [*Jankowiak and Tanré*, 1992; *Swap et al.*, 1996; *Moulin et al*, 1997a; *Husar et al.*, 1997]. These observations offer a remarkable coverage in time and space that was not previously available The Meteosat platform performs wide spectral band imaging of the Sahara and the adjacent oceanic regions in the solar spectrum (visible light spectrometer (VIS)

[1] Also at Institut für Anorganische und Angewandte Chemie, Universität Hamburg, Hamburg, Germany

Paper number 97JD02779.
0148-0227/98/97JD-02779$09.00

plus near infrared channel) and in the thermal infrared useful for detailed dust observations. The dust optical thickness can be retrieved sufficiently quantitatively over oceans from the VIS observations since ocean albedo is low and fairly constant [*Dulac et al.*, 1992a]. The good accuracy obtained allows us to compare in detail modeled dust optical thickness distributions. However, quantitative mass budgets of the dust transport from such images are a challenge. For example, the derivation of aerosol mass from optical thickness requires assumptions on the aerosol particle size distribution, which can hardly be justified for specific events. In addition, dust loads cannot be estimated directly in cloud-covered areas. Attempts to interpolate aerosol mass in cloud-covered regions are prone to large uncertainty [*Dulac et al.*, 1992a; *Moulin et al.*, 1997a].

Since major dust events happen sporadically, any modeling of the dust transport needs to resolve hourly changes in dust fluxes and to simulate several months to cover extreme events and seasonal changes [*d'Almeida*, 1986; *Joussaume*, 1990; *Genthon*, 1992; *Tegen and Fung*, 1994]. The computational limitations have, however, led to simplified treatments, particularly of the aerosol size distribution. Since large particles are removed much faster, a significant change in size distribution is to be expected as the distance from the source increases. Some more explicit work was done incorporating a large number of size bins in two-dimensional (2-D) and mesoscale models [*Schütz*, 1980, *Westphal et al.*, 1988]. The retrieval of geochemical information on dust fluxes and the optical properties of the dust aerosol suffers from model shortcomings which concern the treatment of the size distribution.

Although the models mentioned above were able to capture the general features of dust appearance, their validation is done at best by comparison with very few point measurements. A dynamic system like dust mobilization and transport is not adequately constrained with such few observations. *Nickovic and Dobrivic* [1996] have made an early attempt to validate a dust transport model through comparison with daily satellite pictures. The work presented here tries to close the gap in investigating the dust transport both on the computational and the validation part of the problem. The primary aim was that the numerical code representing the model was efficient enough to simulate the evolution of global mineral dust fields for several years with present-day supercomputers. This goal implied a description of the aerosol size distribution evolution, and the simulations had be validated with daily synoptic data related to the occurrence of aerosol.

We have excluded from this study the incorporation of the wet deposition process. We are aware that wet deposition is the most important process in removing long-range transported mineral dust particles. However, we believe that our simulations, as is shown by the comparison with satellite observations, justify the constrained analysis of dust model components as presented here for a case study.

2. Model Description

2.1. Representation of the Aerosol Size Distribution

One specific problem of a mineral dust transport model is the fact that particles having the same composition differ in size over a range of several magnitudes. Observations of mineral aerosol size distribution show that it is composed of several lognormal distributions [*Shettle*, 1984, *d'Almeida*, 1986; *Jaenicke*, 1987]. To account correctly for the size distribution effect, the model should: (1) allow for the partitioning of mass among several distribution modes; (2) reproduce the gradual change in size distribution during transport; (3) utilize the actual size distribution for calculating fluxes and optical properties and (4) be computationally efficient."

Two different representations of the aerosol distribution have been developed in parallel. One is a computationally efficient spectral scheme, the second one is a bins scheme; discretizing the size distribution, which is more accurate given a sufficient number of size classes. In both schemes, lognormal distributions are used, and it is assumed that a superposition of up to three aerosol modes provides sufficient information on the size distribution [*d'Almeida*, 1986; *Jaenicke*, 1987].

2.1.1. Spectral scheme. In the spectral scheme these three aerosol modes of the mineral dust distribution are described by three independent constant-width lognormal distributions. It is useful to recall at this point that one lognormal distribution is fully described by any three of the four parameters: mass median diameter (*MMD*), geometric standard deviation (σ), mass (m), and number (N). It is important to note here, that the number median diameter (*NMD*) could also be used as one of the four parameters, replacing the mass median diameter where needed. With a constant standard deviation, any two of the remaining three parameters, for example *MMD*, m and N are sufficient to infer the value of the other unknown parameters of the distribution. This results in considerable savings in computing the aerosol distribution evolution in a transport model, because one can use the number and the mass concentration to represent any aerosol mode n. These two parameters constitute two tracers which can be handled independently in the transport routines. The number and mass median diameter are computed at any grid point from the local concentrations of number and mass, considering particle density, assuming a spherical particle shape. For the mineral aerosol we have used a value of ρ_p = 2.65 gm^{-3}:

$$NMD_n = \sqrt[3]{\frac{m_n \cdot 6}{N_n \cdot \pi \cdot \rho_p \cdot \exp(4.5 \cdot \ln^2 \sigma_n)}} \quad (1)$$

$$MMD_n = NMD_n \cdot \exp(3 \cdot \ln^2 \sigma) \quad (2)$$

The assumption of a constant standard deviation implies that the width of an aerosol mode does not vary, but the total mass can take any value for a given median diameter.

2.1.2. Bins scheme. In the bins scheme aerosol mass is handled in independent classes. We have used a variable number of size classes (5-100) with logarithmically spaced intervals covering a particle range from 0.01 to 500 μm. Each bin is characterized by its geometric mean diameter. Size dependent processes are calculated as a function of this diameter. With a large number of size classes this procedure allows us to reproduce the change in size distribution accurately. Our sensitivity tests indicated that 20 bins are sufficient to avoid numerical inaccuracies, for example when distributing mass at the source from a continuous distribution into a limited number of size classes.

In contrast to the spectral scheme an irregular size distribution will evolve with the bins scheme as a consequence of transport and mixing. However, to summarize information we have computed size distribution parameters for diagnostic purposes in a simplified manner:

$$\log(MMD) = \sum m_i \log d_i / \sum m_i \quad (3)$$

$$\log(\sigma_g) = \sqrt{\sum m_i (\log MMD - \log d_i)^2 / \sum (m_i)} \quad (4)$$

To derive averages of the size distribution parameters in the diagnostic process for air mass columns, a mass weighting was applied to exclude inaccurate values from essentially dust free layers.

2.2. Source Term

The inspection of infrared satellite images shows that dust rise can be a localized phenomenon [*Legrand*, 1990]. We have studied the IR images for our case study and searched for supplementary information on potential source regions. Infrared images are also sensitive to the presence of dense transported dust clouds and cannot give information on source location for areas that are covered with water clouds. In our case, IR images are not as unambiguous as one would like them to be, because of a varying cloud cover in the time period under study. However, the origin of the dust clouds moving toward the Mediterranean seemed to be located in the center of west Africa There the Taoudeni basin has been identified earlier as an important dust rise region [*Legrand*, 1990, *Bergametti*, 1992]. Surprisingly, one grid box alone centred at 23°N and 2.5°W (about 300x300 km^2) proved throughout our different simulations to be a good assumption of the active source, being responsible for a good portion of the dust cloud observed over the Mediterranean and also over the Atlantic.

A source formulation needs not only to include a choice of the spatial distribution of the source but also of the source strength, an initial aerosol size distribution, and a modulation by surface wind and diurnal changes. Since we are not intending to derive a mechanistic model of the source function, we resort to simplified assumptions. The good results obtained with our simple source model justify this choice. However, for the sake of completeness, we implemented also a detailed source [*Marticorena and Bergametti*, 1995] in a sensitivity simulation.

Theoretical studies as well as studies in wind tunnels [e.g., *Shao et al.*, 1993] have shown that the upward dust flux is proportional to the third power of the friction velocity. We have assumed as a simplification that the friction velocity is directly proportional to the wind speed. The frequency and intensity of the dust flux also depends on a threshold velocity. We noticed that the surface winds in the source region ranged frequently up to but not higher then about 7 m-s in the period studied. Since dust has risen in the region, we initially have used for the reference simulation a relatively low threshold wind velocity of 3 m-s. However, we have given special attention to this problem in two sensitivity simulations to be discussed below.

The source strength was chosen such that the simulated optical thickness was equal to the observed one from Meteosat over the marine cloud-free Mediterranean Sea during the last days of our case study (July 4-10, 1988). All together the dust flux F_s was estimated to be of the order of 17×10^6 during 16 days. The source emission factor X_s was then 2 [$\mu g\ s^2\ m^{-5}$].

$$F_s = X_s u^3 X_d(t) \quad (5)$$

A frequent observation of dust storms has shown that most dust is observed in the early afternoon [*Bérenger*, 1963; *Middleton*, 1985; *Goudie and Middleton*, 1992]. In an attempt to investigate the importance of the diurnal cycle, we amplified this cycle of the source strength by superimposing a sinusoidal function $X_d(t)$ with a maximum at 15 hours local time, suppressing dust emission in the night.

The mass flux is right away redistributed among the aerosol modes and/or bins according to an initial source aerosol size distribution. *Shettle* [1984] has tried to summarize measurements of size distributions encountered during a dust rise event and after some time of transport. However, the initial size distribution to be chosen for the model needs to be representative of source grid boxes. In our model these boxes have a considerable extent in height (400 m) and area (300x300 km^2). To our knowledge a profile of mass and distribution was never thoroughly characterized by measurements for heights up to 400 m. We have even less information on the coarse particles for which a large vertical mass gradient is to be expected, as a consequence of the immediate removal by sedimentation. The coarse aerosol mode is therefore of minor importance when we want to describe the initial size distribution available for long-range transport. We resorted to *Shettle's* background size distribution. However, *Dulac et al.* [1989] for example as well as our sensitivity studies suggest that the major second mode has a much smaller standard deviation then originally reported by *Shettle* The size distribution used for our reference simulation is found in Table 1.

After conversion of the dust emission flux to aerosol mass, we partition mass as follows: In the bins scheme the aerosol mass m_i in any bin i is computed by integration for the size interval from $d_{i,l}$ to $d_{i,u}$, taking into account that n aerosol modes contribute to the mass:

$$m_i = \sum_n m_n \cdot \frac{1}{2} \cdot \left| erf\left(\frac{\ln d_{i,l} / MMD_n}{\sqrt{2} \cdot \ln \sigma_n}\right) - erf\left(\frac{\ln d_{i,u} / MMD_n}{\sqrt{2} \cdot \ln \sigma_n}\right) \right| \quad (6)$$

With the spectral scheme the aerosol mass injected in any mode is found from the mass fraction the aerosol mode has in the source size distribution. However, we do also calculate the particle number transport. For initialization we need therefore to calculate the number concentration N_n of any aerosol mode which corresponds to the emitted mass m_n of the source size distribution:

$$N_n = \frac{m_n \cdot 6 \cdot \exp(4.5 \cdot \ln^2 \sigma_n)}{\pi \cdot \rho_p \cdot MMD_n^3} \quad (7)$$

Table 1. Aerosol Mass Size Distribution at the Source for Reference Simulation

Mode	*MMD*, μm	σ	Mass fraction, %
1	42.3	1.89	21.9
2	2.52	2.00	78.1
3	0.011	2.13	$2.6\ 10^{-4}$

2.3. Transport

The transport model used is an off-line 3-D tracer transport model (TM2) developed by *Heimann* [1995] and first described by *Heimann and Keeling* [1989]. It solves the continuity equation for the conservation of mass. The tracer transport is driven by analyzed wind fields of the European Center for Medium-Range Weather Forecasts (ECMWF), ensuring that model results can be compared directly to observations. For the period studied here, winds and convection were obtained for every 6-hour-interval. Advection in the model is computed using the slopes scheme of *Russel and Lerner* [1981]. Although it is mass-conservative, the scheme may produce negative concentrations when large concentration gradients coincide with small air mass transports. This was avoided by limiting the slopes. Subgrid-scale vertical exchange processes include turbulent diffusion [*Louis*, 1979] and mass fluxes associated with convective activity. Both are inferred from ECMWF fields of temperature, humidity, and surface evaporation fluxes [*Tiedtke*, 1989].

The vertical spacing in the model consists of nine levels following sigma coordinates on which the 15 level ECMWF data have been interpolated. The six bottom levels of the model remain well within the troposphere. *Ramonet* [1994] incorporated in the model the possibility of using a refined horizontal grid of 2.5°x2.5°. In this resolution, advection is calculated with a 1 hour time step.

This higher-resolution version was used for simulating the Saharan dust transport. The model region chosen for this study included only the area where the geochemical fate of Saharan dust would most probably be contained (see area shown in Figure 1). A natural southern boundary is the

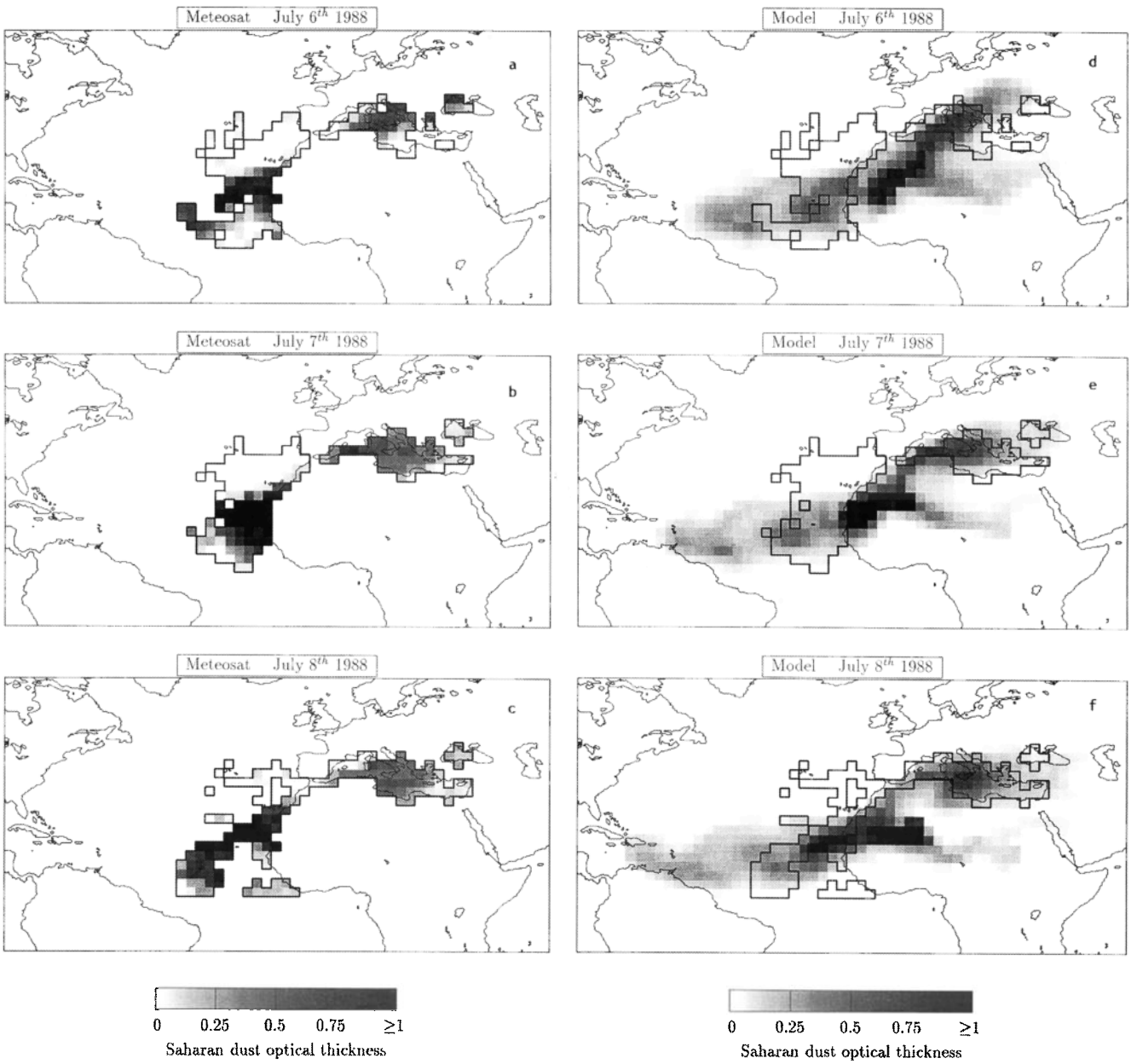

Figure 1. (a-c) Dust optical thickness (at 550 nm) for marine cloud-free area from satellite observations averaged within the model grid. Marine cloud-free area with satellite observations is encircled with a bold line. (d-f) Dust optical thickness (at 550 nm) as simulated by our tracer model. For comparison, the area with satellite observations is also encircled here with a bold line.

intertropical convergence zone where most of the dust is removed by frequent and heavy convective rains. The limited lifetime of the relatively coarse mineral aerosol and the increased precipitation in midlatitude bands suggest further that only limited transport is expected northward of North America, mid-Europe, and mid-Asia.

2.4. Sedimentation

Settling velocities v_T of aerosol particles for a given diameter were calculated according to Stokes relationship, including their dependence on the lower air viscosity at higher altitudes [*Seinfeld*, 1986]. With the bins scheme the mass transfer due to sedimentation of any aerosol size class is simply the product of settling velocity for the geometric mean diameter and time step.

The spectral scheme requires that we integrate the nonlinear sedimentation process for the whole spectrum to accurately calculate fluxes and the transformation of the size distribution. *Slinn and Slinn* [1980] have shown that this transformation can be computed taking into account a characteristic particle diameter and the standard deviation of the distribution. The characteristic number and mass size spectrum these diameters are the mass and number median diameter for every aerosol mode, respectively. *NMD* and *MMD* thus have to be calculated with the spectral scheme at every time step in all grid boxes (see (1) and (2)). The mean settling velocity of mass and number of any aerosol mode is then to be found by

$$\bar{v}_{T,mass} = v_{T,MMD} \cdot \sigma_n^{2\ln\sigma_n} \tag{8}$$

$$\bar{v}_{T,number} = v_{T,NMD} \cdot \sigma_n^{2\ln\sigma_n} \tag{9}$$

The large range of settling velocities poses computational problems with regard to two effects: First, numerical diffusion can artificially increase the vertical mixing with considerable effects on transport and aerosol residence times. Second, multilayer crossing of large particles may occur for large time steps typically used in large-scale models. We calculate thus the sedimentation fluxes of mass in every size class (in the bins scheme) and mass as well as number of a given mode (in the spectral scheme) in strict analogy to the vertical advection routine The numerical diffusion is effectively minimized using the slopes scheme of *Russel and Lerner* [1981]. The fluxes $F_{l,k}$ from any grid box l to a grid box k below are computed by accumulating all dust fluxes arriving at layer k from the layers above to derive new mass (and number) concentrations. The sum of mineral dust arriving at the surface constitutes the deposition flux.

2.5. Modeled Aerosol Optical Thickness

Relating the aerosol mass to optical thickness requires the aerosol specific extinction cross section, which depends strongly on particle diameter and refractive index. The refractive index of mineral dust aerosol has been chosen to be 1.50 - 0 01 i, a result obtained independently by *Moulin et al.* [1997b] and by *Ignatov et al.* [1995] when comparing Sun photometer and satellite-derived optical thickness. Any possible dependence of the refractive index on particle diameter, particle shape, or other factors such as humidity is beyond the scope of our simulation.

However, the dependence of optical thickness on particle diameter is well described by Mie -theory. We calculated dust optical thickness (τ_{aer}) at 550-nm wavelength, which corresponds to the Meteosat VIS channel in every model grid column, assuming single scattering and accounting for variations in the dust size distribution in the column:

$$\tau_{aer} = \sum_{n,l} K^*_{550}(MMD_{n,l}, \sigma_{n,l}) \cdot m_{n,l} \tag{10}$$

The aerosol specific extinction cross section ($K^*_{550}(MMD_{n,l}, \sigma_{n,l})$) was precalculated using Mie theory as a function of aerosol size distribution parameters for a lookup table (13x13) of K^*_{550} values corresponding to pairs of the two aerosol size distribution parameters in the range of 0.01-50 μm for the *MMD* and in a range of 1 7-3.5 for the standard deviation and the above mentioned refractive index and a particle density of 2.65. In the diagnostic process of the model output the aerosol specific extinction cross section in any grid box of layer l was derived by a bicubic spline interpolation from this lookup table for the aerosol spectrum of each mode

3. Model Validation Procedure

3.1. Satellite-Derived Aerosol Optical Thickness over the Ocean

For comparison we have used images in the visible spectrum (VIS, 0.35-1.1 μm) as taken by Meteosat-2 satellite imager. To obtain high signal to noise ratios, images taken at noon (1130-1200 UTC) were considered. The area of possible comparison ranged in longitude from 40°W to 40°E and in latitude from 5°S up to 45°N Images were processed as described by *Moulin et al.* [1997a] on the basis of numeric counts of subsampled International Satellite Cloud Climatology B2 images. Cloud contaminated pixels were identified over the oceans by checking against a local variance and an absolute threshold. Pixels were marked as being cloudy, associated with patchy cloud fields, if the variance of the enclosing 3x3 pixels were greater than four numerical counts. The absolute threshold, associated with a large cloud cover in the cell, was set to be 64. An atmospheric radiative model was then used to account for the backscatter from the sea surface, the attenuation by gaseous absorption, and the molecular backscatter from a standard atmosphere to retrieve the leftover, aerosol radiance [*Tanré et al.*, 1990]. The absolute calibration of the sensor and seawater reflectance was taken from *Moulin et al.* [1996]. Taking into account aerosol optical properties, we derived the dust optical thickness at 550 nm over the oceans. We used the background desert aerosol model of *Shettle* [1984] (size distribution as in Table 1, but with $\sigma_2 = 3.2$). Observations in the Atlantic region indicate some variability in size distribution parameters. However, it should be emphasized that the retrieval of dust optical thickness from the broad spectral band of the Meteosat detector is not very sensitive to variations of the assumed aerosol size distribution [*Moulin et al.*, 1997b], whereas the calculation of optical thickness in the transport model for the wavelength 550 nm is much more sensitive to the modeled size distribution as discussed below. A smaller standard deviation of $\sigma_2 = 2.0$ as used in the transport model changes the satellite-derived optical thickness by not more than 2%. The identical refractive index was used for satellite

retrieval and the model simulation of optical thickness. The relative accuracy in estimating the optical thickness for a single pixel was estimated to be on the average +/- 25% by comparison with ground-based measurements [*Moulin et al.*, 1997b].

Whereas the calculation of the aerosol optical thickness is relatively straightforward, any estimate of the aerosol mass from satellite observation involves further uncertainties. Fine particles dominate the backscattered signal; relatively larger particles dominate the mass. The change in aerosol radiance is thus less representative for significant changes in the total aerosol mass. Since the model was designed to predict the aerosol distribution at any given point and thus would be able to compute optical thickness, comparison with the transport model was done on the basis of optical thickness.

3.2. Comparison of Satellite / Model Values

For direct comparison with modeled aerosol optical thickness all marine, cloud-free pixels falling into one grid element of the model were averaged. This could be composed of up to 100 individual pixels. Because a potential source of error in satellite-derived optical thickness are undetected clouds, we only use those grid elements where the marine cloud-free area fraction was larger than 20% in our statistical analysis. In the correlation analysis we also included areas where the optical thickness was below the detection limit of the satellite captor ($\tau_{aer} < 0.1$). This improves correlation for example in the Mediterranean region, because the correlation coefficient reflects the quality of the simulation of both dust-free and dusty areas. This contrast is well reproduced by the model, despite the lack of accuracy of low values of optical thickness.

Corresponding to these satellite observations, simulated 3-D fields of mineral dust were processed with a diagnostic tool, which we developed to compute mean aerosol properties for a region of choice. Some of the information such as deposition, mass loads, and vertical gravity center of the dust mass needed only simple processing. However, some aerosol properties, like size distribution parameters and optical thickness, need to be explicitly computed for every grid box to aggregate meaningful column values and mean values for any area of interest. Statistical procedures could then in a final step be applied to compare the modeled fields with satellite observations for just the marine cloud-free area.

4. Reference Simulation of Case Study June-July 1988

A 16-day period from June 25 to July 10, 1988 was selected for an intensive study. In this season the satellite sensor is most sensitive to dust, because the scattering angle is close to 180°. The last days were essentially cloud-free at least over the Mediterranean, and no rain was observed in this region. Several remarkable dust plumes were observed over the Mediterranean and the Atlantic.

For selected days the distribution of the dust optical thickness retrieved from satellite pictures is shown in Figures 1a-1c. We would like to draw attention to July 6, when a distinct plume develops and crosses the whole Mediterranean to the northeast, associated with a maximum in optical thickness. This northeastward transport in a narrow plume typically occurs with a cyclone off Portugal and an anticyclone centered over the central Sahara. ECMWF surface winds in the source area were highest June 21, 28, and 30, well before the plume arrived over the Mediterranean. Even more prominent is the dust plume over the Atlantic in the trade wind region.

The result of the simulation A is shown for the same days in Figures 1d-1f. Especially over the Mediterranean we observe a remarkable similarity of simulation and satellite observation. The good agreement with the satellite at noon implies that the model is capable of simulating the transport reasonably well over a timescale of less than a day. A high correlation based on daily values for all marine and essentially cloud-free grid elements for the period July 4-10 is found between retrieved and simulated optical depths (r=0.86) in the Mediterranean area; over the Atlantic a somewhat lesser agreement (r=0.78) is found. The comparison between satellite and simulation is presented on a point-by-point basis in Figure 2. For the remote western Atlantic (see Figure 4 for the definition of the area) the correlation is worse. We suggest that the steady trade wind transport pattern is responsible for the correlation over the Atlantic. Any dust which has been simulated to disperse and enter the air masses associated with the trade winds will be transported along with them, leaving areas to the northwest free of dust. This will produce correlation between simulated and observed optical thickness especially over the coastal Atlantic. Shifting winds in the source region have resulted in the transport of dust to western Africa and hence to the trade wind regime and also from our single-grid box source during our 16-day period. Such a shift in major transport direction can also be seen in Figures 1d-1f where the dust cloud over the Mediterranean gets separated from the one over the Atlantic. The relative smaller values of simulated optical thickness over the Atlantic indicate that additional dust source regions have been active in the period studied.

Observation and simulation show the arrival and dispersion of the dust cloud in the Mediterranean area (Figure 3) with a maximum in optical thickness occurring over the western Mediterranean on the July 6, reappearing 2 days later over the eastern basin, a delay readily explained by the required transport time in westerly winds. The observed and simulated slightly lower optical thickness over the eastern basin can be explained by the en route removal and dilution of dust. The coincidence of the day-to-day variation and the correlation coefficients of the daily comparison support strongly the choices made for the source location.

However, a quantitative agreement about optical thickness requires further assumptions on the source strength and the size distribution. As a starting point, we have chosen in sections 2.2 reasonable values for these parameters. To reproduce the average optical thickness of 0.21 observed by Meteosat over the Mediterranean Sea requires a source flux of 17.3 10^6 t in the 16-day period. D'*Almeida* [1986] estimated the monthly Saharian dust flux for the 2 months of June and July in 1981 and 1982 to range between 42 and 93x10^6 t. A slightly changed combination of the size distribution parameter values would also provide a solution to the problem. However the range in which one can choose the values of σ, *MMD*, and the emission flux of the major mode is limited as will be shown by our sensitivity simulations.

Figure 4 summarizes the mass budget in that part of the model domain where satellite observations are available.

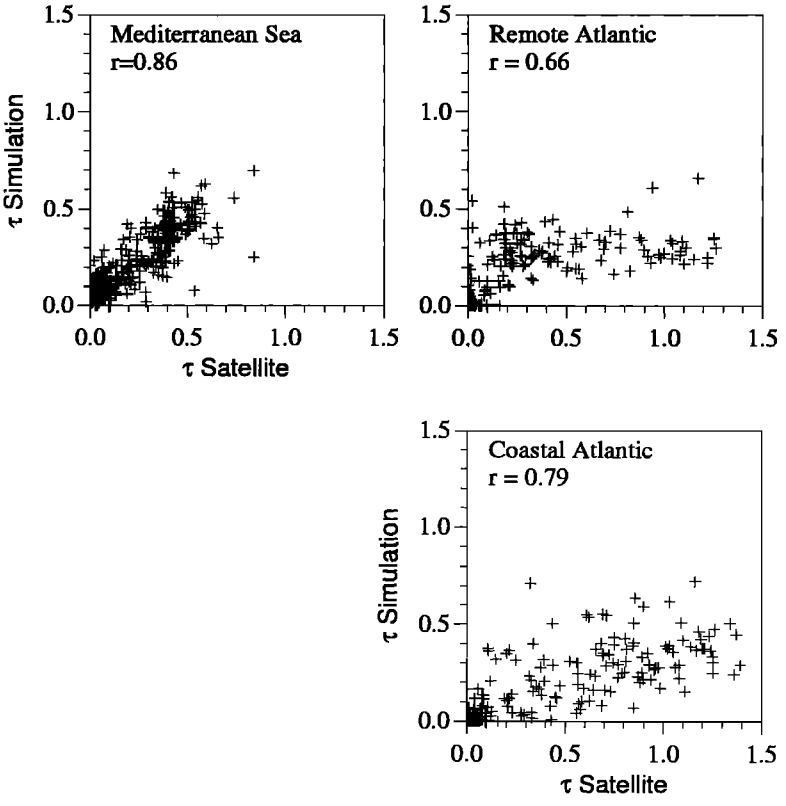

Figure 2: Point-by-point comparison of observed and simulated optical thickness over the whole Mediterranean Sea, and the coastal as well as remote Atlantic as marked in figure 4.

Significantly more dust is transported into the Atlantic region. Only a very small portion of the total emitted dust arrives over the Mediterranean. It is remarkable that the agreement in dust plume position between simulation and satellite is based on just this small fraction of the transported dust. The large deposition flux over Africa points to the importance of the sedimentation process. While almost all of the coarse mode aerosol is removed, 30% of the major mode aerosol mass is also lost over the Sahara.

The change in size distribution is an important new element of our study. The evolution of the mass and number size distribution during transport is shown for three selected areas on the way from the source to the Mediterranean in Figure 5. Column mass loads were computed for 3x3 grid boxes at the source, 500 km northeast on the track to the Mediterranean and around Corsica, on the days with maximum values of mass loads. Both the numerical and the spectral schemes predict the vanishing of the coarse mode, a substantial shift to smaller diameters, and the predominance of the major mode. The occurrence of a substantial coarse fraction on July 1 is probably due to rapid transport from the source region and has been simulated with both schemes.

Only very few data are available to validate the predicted vertical distribution in the atmosphere. However, some information on dust transport was gathered on the importance of the so called Saharan air layer aloft transporting dust. This was obtained through careful interpretations of red rains and dust events remote form the source, for example in middle Europe, by looking at temperature and humidity profiles and 3-D backward trajectories [*Reiff et al.*, 1986; *Dulac et al.*, 1992b]. By this method the dust layer observed over the Mediterranean during the June-July 1988 period was thought to be between 3 and 5 km thick. The comparison between the dust movement as deduced from hourly series of Meteosat images and the vertical wind field as deduced from a rawinsonde profile indicated that the dust layer was at an average altitude of about 2300 m on July 5 over Corsica [*Dulac et al.*, 1996]. The evolution of the measured temperature profiles over the Mediterranean confirms a Saharan air layer and its descent in the course of the passage of a front to the north after July 6. The simulated vertical aerosol profile consists of a dust layer with a gravity center at 3900 m on July 6 over the western Mediterranean, showing a similar descent after July 6 with a minimum on July 9 at 2700 m. This indicates that the vertical redistribution is well simulated and might be one of the key factors which allowed us to reproduce the dust event.

5. Sensitivity Studies and Discussion

Not all components of the model are equally important for the reproduction of the dust plume. We therefore performed 14 sensitivity simulations (named C through O and Z) summarized in Table 2. We compared each of these simulations to the reference case just described in order to study the effect of the numerical scheme, the size distribution, the source location and its diurnal cycle, subgrid processes and the averaging of ECMWF fields. Both the experiments with the spectral (A) and the bins scheme (B) were regarded as reference simulations. The discussion is based on the direct

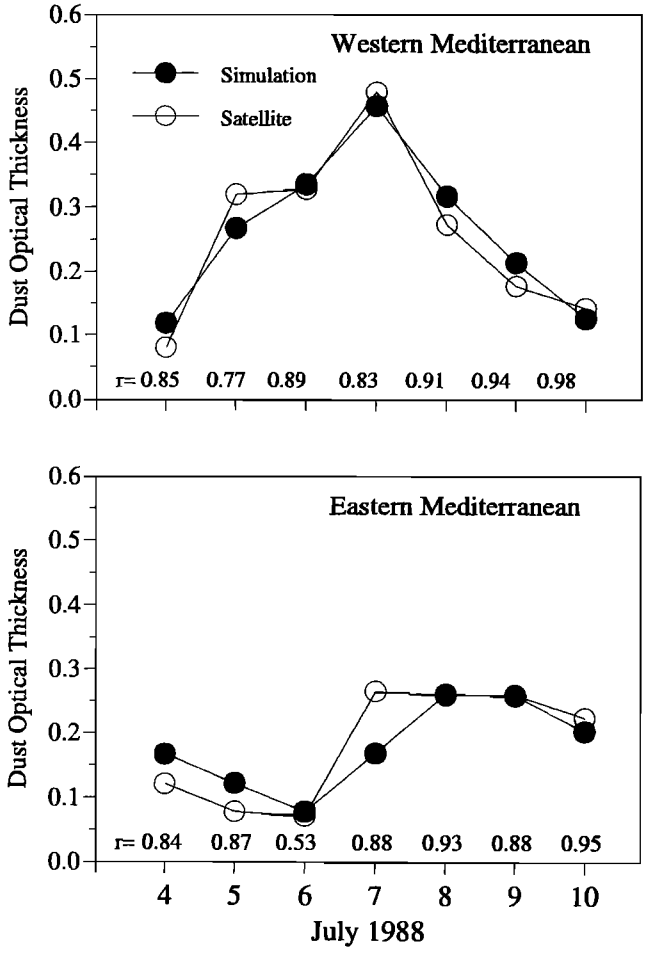

Figure 3. Dust optical thickness and daily correlation coefficients from comparison with satellite observation for the western Mediterranean (N = 18 grid box elements) and the eastern Mediterranean (N=24).

comparison with satellite-derived optical thickness mainly over the Mediterranean Sea. The source strength in all experiments was kept constant.

There are two major features of the atmospheric dust transport, which we use to group our sensitivity simulations: (1) The reproduction of the position of the dust cloud serves to evaluate the model transport and dispersion characteristics. The correlation coefficients of the comparison satellite model for selected regions are a good measure for this feature. As can be seen from Table 2, most significant degradation of the dust plume simulation is found in experiments G, I, L, N, and O. (2) The correct absolute value of simulated optical thickness would indicate a good simulation of both the vertically integrated aerosol mass and the aerosol size distribution. This feature is much more difficult to reproduce and validate since it requires a comprehensive and quantitative understanding of the dust transport. Optical thickness from simulations E, H, I, L, and N are noticeably reduced from the reference simulations, and they are significantly increased in simulation D, but also the rest of the simulations show scatter with regard to this parameter. Relative differences between the simulations allow us to judge the influence of different processes on the overall magnitude of the dust transport.

5.1. Sensitivity to Numerical Treatment of Size Distribution

Both numerical schemes developed here have an explicit treatment of the size distribution. Whereas 1 day of simulation with one major aerosol mode and the spectral scheme requires 21 cpu on a Cray C90 supercomputer, the same simulation with the bins scheme (20 tracers) required 5 times more cpu. This is the motivation to develop a more detailed comparison of the schemes and the numerical procedure to handle sedimentation, which is the important process transforming the aerosol size distribution in our model.

Comparing the reference simulations A and B, both give similar correlation coefficients over the Mediterranean and over the eastern Atlantic. We conclude that the position of the dust cloud is well described by both the spectral and the bins scheme and thus is not sensitive to the numerical scheme.

The assumption of a constant standard deviation used for the spectral scheme is the most critical one. Owing to the size dependent removal effects any lognormal distribution is transformed during transport to a distorted distribution with a smaller σ. The accurate bins scheme may be used to assess this effect. While the standard deviation of the major mode decreases slightly in simulation B, it drops considerably in

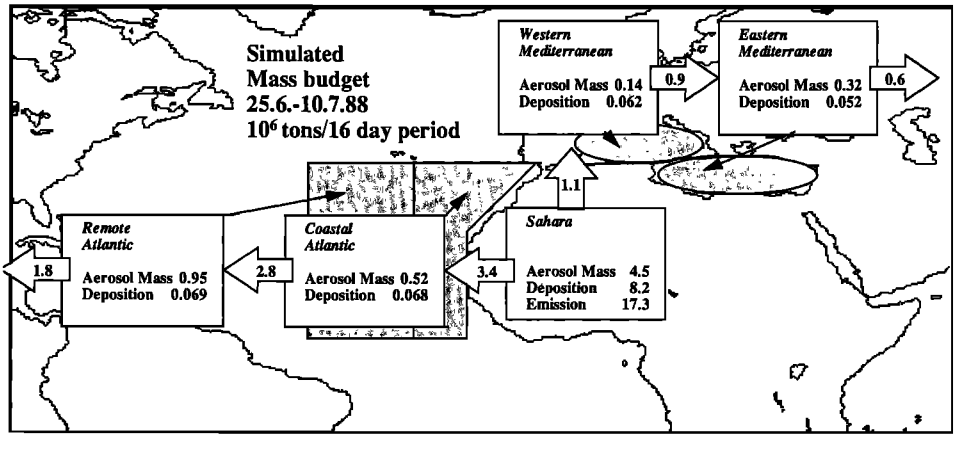

Figure 4. Overall mass budget of the reference simulation, assuming an initial size distribution as described in table I and an adjustment of the source strength by comparison with the satellite observations of the 4th to 10th July over the Mediterranean Sea.

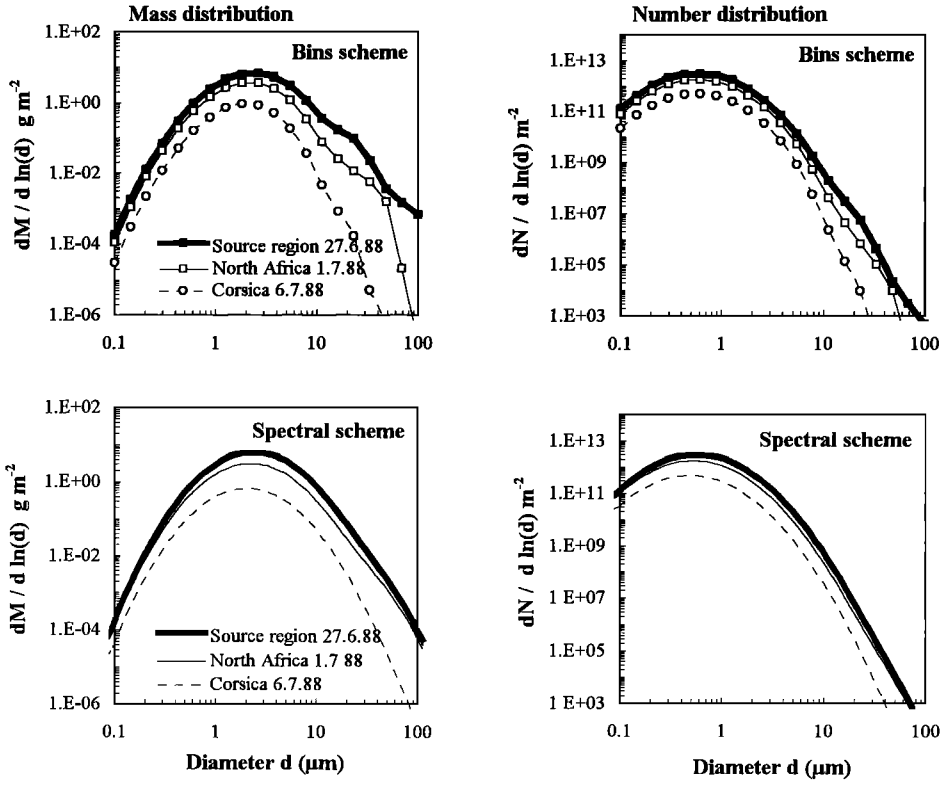

Figure 5. Simulated aerosol size distributions over the source, en route over Africa and over the Mediterranean Sea, with the bins and the spectral scheme.

Table 2. Sensitivity Simulations Performed for the Period June 25 to July 10, 1988

Run	Description	Scheme	τ	r
	Reference Simulation and Accuracy			
A	spectral scheme, background dust model [*Shettle*, 1984] three aerosol modes but σ_2=2.0, one grid box source area	spectral	0 169	0.86
B	bins scheme, 20 bins	bins	0.210	0 86
	Sensitivity to Size Distribution			
C	major aerosol mode alone	spectral	0.169	0.86
D	bins scheme, σ_2=3.2, *Shettle*'s [1984] background dust model	bins	0.323	0.86
E	aerosol distribution "wind carrying dust" *d'Almeida*, 1987]	spectral	0 007	0 85
	Sensitivity to Numerical Treatment of Sedimentation			
F	time step decreased tenfold for sedimentation routine	spectral	0.164	0.86
G	no slopes recalculated in sedimentation subroutine	spectral	0.247	0.57
	Sensitivity to Source Location			
H	larger source, increased by eight surrounding grid elements	spectral	0.131	0.87
I	shift of source area 5° to the west	spectral	0.077	0.79
J	no diurnal cycle superimposed on source function	spectral	0.153	0.86
K	threshold velocity increased to 6 m-s	spectral	0.189	0.86
Z	mechanistic model from *Marticorena and Bergametti* [1995]	spectral	0.279	0.70
	Sensitivity to Subgrid Processes			
L	no convection, no vertical diffusion	spectral	0.021	0.55
M	no vertical diffusion but convection	spectral	0.161	0.85
N	no convection but vertical diffusion	spectral	0.085	0.80
	Sensitivity to Averaging of ECMWF Wind Fields			
O	24hour interval for wind field reading	spectral	0.211	0.82

Optical thickness τ and correlation coefficients r are from comparison with satellite observations for the whole Mediterranean Sea area, July 4-10, 1988. Note that the source strength was equal to 17 Mt., with the exception of simulation Z (50 2 Mt.).

simulation D from 3.2 to 2.3 (Table 3). Figure 6 summarizes a series of simulations where the standard deviation was varied with both schemes. The results converge when σ decreases. With a standard deviation of σ=2.0 the difference in simulated mean optical thickness between the bins and the spectral scheme is then 19% over the western Mediterranean and 21% over the eastern Atlantic. As is discussed in section 5.2 , a choice of a small standard deviation of σ=2.0 is also suggested by measurements and mass balance arguments. With the advantage of being able to use the spectral scheme, it seems thus justified to use a constant standard deviation for a dust aerosol distribution of 2.0.

5.2. Sensitivity to the Aerosol Size Distribution

An explicit and detailed treatment of the dust size distribution has not been implemented, to our knowledge, in any other model of this scale. It is thus of interest to study the overall performance of the dust model with respect to the variation of the distribution parameters. Table 3 shows the simulated size distribution in the receptor area of the Mediterranean Sea and optical properties of the dust cloud there. To relate this to the mass balance in the different simulations, we choose to calculate the mass fraction deposited close to the source over Africa and the simulated mass load over the Mediterranean Sea.

It is currently deemed necessary to use at least three aerosol modes to represent the size distribution. However, only one major mode, which is centered around 2 μm, is needed to reproduce the long-range transport and dust optical thickness over the ocean. This can be inferred from sensitivity simulation C, where the coarse and very fine aerosol modes were omitted. It should be stressed, however, that this conclusion comes from the use of optical thickness as validation parameter. A validation based upon deposition fluxes would have stressed the importance of the coarse mode.

The choice of the distribution parameters of the major mode critically affects the mass balance in the model region. The initial standard deviation and mass median diameter of the source aerosol determine the rate with which the aerosol size distribution is transformed by sedimentation. Increasing either one of these parameters increases the sedimentation flux close to the source. However, a distribution with a larger initial standard deviation contains both more coarse and more very fine aerosol particles. The latter settle very slowly and limit the mass to be removed by sedimentation. Simulation D, having a size distribution as proposed originally by *Shettle* [1984] as background dust distribution, consequently shows slightly higher deposition in the Sahara region and after long-range transport a much finer aerosol (*MMD*, 1.3 μm) over the Mediterranean Sea when compared to the reference simulation B.

The introduction of a source size distribution with a larger mass median diameter produces a dramatic difference. For an intermediate distance from the actual dust rise zone, *d'Almeida* [1987] proposed an aerosol distribution named "wind-carrying dust." For the major mode a *MMD* of 14.7 μm is assumed. This choice increases the deposition everywhere in the model region and leaves very little aerosol mass for long range-transport (simulation E). A larger mass median diameter (2.53 μm) over the Mediterranean represents a memory of the initially larger aerosol. Measurements done in

Table 3. Evolution of Size Distribution, Mass Balance and Optical Properties

		Size Distribution of Mediterranean Sea July 4-10,1988		Deposition of Sahara June 25 to July 10,1988	Mass Load of Mediterranean Sea July 4-10, 1988	Optical Properties of Mediterranean Sea July 4-10, 1988	
Run	Short Description	mmd, μm	σ	%	$g\ m^{-2}$	τ	$K^*_{550}, g^{-1}m^2$
				Reference Simulation and Accuracy			
A	spectral scheme	2.03	2.00	55.8	0.176	0.169	1.04
B	20 bins scheme	1.86	1.78	47.6	0.219	0.210	1.04
				Size Distribution			
C	major aerosol mode	2.02	2.00	44.1	0.176	0.169	1.04
D	bins scheme, σ_2=3.2	1.30	2.33	51.2	0.205	0.323	0.63
E	dust *d'Almeida*	2.53	2.10	95.8	0.009	0.007	1.29
				Treatment Sedimentation			
F	time step decreased	1.99	2.00	47.3	0.167	0.164	1.01
G	no slopes	2.27	2.00	40.5	0.295	0.247	1.19
				Source Location			
H	source enlarged	2.05	2.00	54.2	0.138	0.131	1.05
I	source area to west	2.09	2.00	54.4	0.083	0.077	1.08
J	no diurnal cycle	2.02	2.00	55.0	0.159	0.153	1.04
K	threshold 6 m-s	2.00	2.00	47.1	0.194	0.189	1.02
Z	mechanistic model	2.01	2.00	49.0	0.282	0.279	1.01
				Subgrid processes			
L	no subgrid exchange	1.42	2.01	78.4	0.015	0.021	0.74
M	only convection	1.94	2.00	64.3	0.158	0.161	0.99
N	only vertical diffusion	1.90	2.00	62.8	0.082	0.085	0.97
				ECMWF Wind Fields			
O	24-hour fields reading	1.94	2.00	59.9	0.209	0.211	0.99

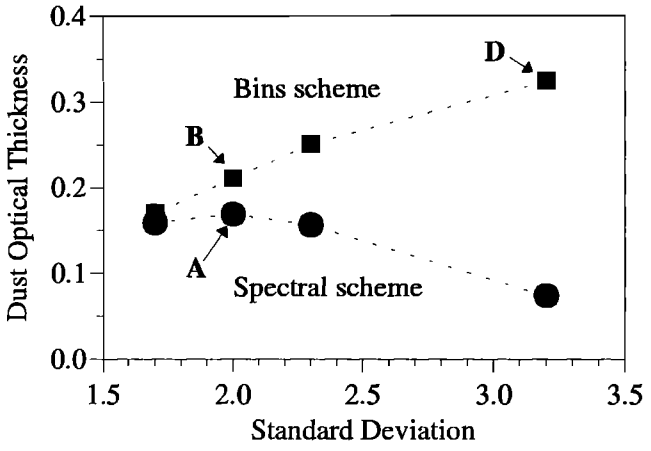

Figure 6. Simulated average dust optical thickness over the western Mediterranean for July 4-10 as a function of the standard deviation of the major dust mode from corresponding bins and spectral scheme simulations.

Corsica show *MMD*'s between 2.0 and 2.3 during dust events [*Dulac et al*, 1989]. Thus both simulations D and E fail to reproduce the size distribution observed over the Mediterranean. Moreover, with *d'Almeida's* [1981] size distribution the source strength would need to be 520×10^6 t in the 16-day period to reproduce the satellite derived-values. This is clearly unrealistic.

Not only do different size distributions affect the mass balance of dust, but the aerosol properties are also changed. As shown in Table 3, the conversion factor K^*_{550} from aerosol mass to optical thickness can vary by a factor of 2. Comparing simulation B and D reveals that with almost the same simulated aerosol mass load but significantly smaller particles in D optical thickness may change by a factor of 1.5. The comparison with satellite observations on the basis of optical thickness is thus highly justified.

5.3. Sensitivity to Numerical Treatment of Sedimentation

The model treatment of the sedimentation process may cause considerable numerical diffusion in the vertical dimension. This also affects the transport and transformation of the size distribution. If the z slopes are not recalculated during the sedimentation process (simulation G), large aerosol particles stay at high altitudes, once they are brought up by convection The vertical gravity center of dust over the Mediterranean increases to 5.3 km compared to 3.3 km in A. Simulation G thus shows significantly less deposition near the sources as compared to the reference run. More serious is the substantially degraded correlation with satellite observations over the Mediterranean. A change in the vertical redistribution of the dust, by treating the sedimentation as a simple Euler-forward process, leads to an incorrect simulation of the long-range transport. This underlines that a higher-order numerical scheme needs to be introduced for the sedimentation process.

The spectral scheme is even more sensitive to the sedimentation scheme. The explicit calculation of the mean settling velocity overestimates the actual settling. In an attempt to increase the accuracy for the spectral scheme, we have decreased the time step for invoking the sedimentation routine tenfold (simulation F). This makes the spectral scheme calculation look like the accurate bins simulation B also in absolute value of optical thickness. The decrease in time step, however, involves a large increase in cpu time, which means there is no advantage to this scheme over the bins scheme.

A disadvantage of the spectral scheme is that any deviation from the lognormal distribution during transport cannot be treated. In the case of multiple source areas, aged aerosol is mixed with any freshly injected aerosol, which in nature would produce a multiple mode size distribution but recombines in the spectral scheme to a weighted average lognormal distribution.

5.4. Sensitivity to Source Location

We found that a single grid box source over central west Africa can be used to simulate the dust cloud evolution over the Mediterranean Sea. Increasing the source area (H) by the surrounding eight grid elements does not improve the correlation coefficient. The decrease in optical thickness over the Mediterranean, with the identical overall dust emission flux, indicates that the mass is spread and dispersed to other regions, for instance, the Atlantic.

This fits well with the idea that other source areas may be important in providing additional dust to the Atlantic plume. A shift of the source area only 5° to the west (I) favors the dust transport into the trade wind regime. The agreement between satellite-derived and simulated optical thickness over the Atlantic is slightly improved (not shown). More significantly this shift deteriorates the correlation over the Mediterranean Sea. Consequently, additional dust sources responsible for some part of the dust clouds over the Atlantic must have been more to the west.

We also tested the importance of the diurnal cycle for the evolution of the dust plume during long-range transport. In simulation J we omitted the modulation of the diurnal cycle as described in the source section with no major change to the quality of the simulation. We suppose that the diurnal signal is smeared out during long-range transport in the relatively coarse grid. However, this change in the diurnal cycle of the dust rise reduces the simulated optical thickness by 10% over the Mediterranean.

We also tested the sensitivity to the timing of the source. The long-range transport requires that the simulation starts at least on July 1 to simulate the dust appearance on July 4-10 over the Mediterranean. A later initialization drops the correlation with satellite observations (not shown). This underlines the need for at least 10 days of simulation to capture the development of a dust cloud and hence the necessity of a computationally efficient large-scale model to simulate the dust transport.

Another experiment, which affects the timing of source activation, was done by applying a threshold velocity for dust rise of 6 m-s (simulation K). Then 65% of the simulated dust injection occurs on the June 21, 28, and 30, whereas this quota is only 38% for the reference simulation. Also, in this experiment the simulated dust plume positions do not change, and correlation remains high. However, the optical thickness increased by 10% over the Mediterranean. This reflects albeit an identical emission flux over the whole period; the different transport occurring on different days will determine the dust loading arriving over the Mediterranean. In our case K, dust rise appears only on days with higher winds, which are

associated with more vertical mixing and thus a higher probability for the dust to be transported long range.

Simulation Z includes the most advanced mechanistic source model of Marticorena and Bergametti [1995]. The dust emission in the western Sahara with this scheme was 50.2 megatons (Mt) in 16 days. This increase in dust emission leads to the increase in optical depth over the Mediterranean Sea However, the dust pattern as derived from this simulation and its correlation with the satellite observations do not improve over the reference simulation. This confirms that we have, indeed, identified the relevant source for our case study, which is obviously more difficult to achieve with a general source model such as the one of Marticorena and Bergametti.

5.5. Sensitivity to Subgrid Processes

The vertical distribution is strongly dependent on the inclusion of convection. Without convection the aerosol remains at altitudes corresponding to the first and second model layer up to approximately 1000 m. A simulation with neither convection nor vertical diffusion had the most drastic effect on the long-range transport (L). The importance of convection rather than vertical diffusion can be seen from simulations M and N. Only simulation M, without vertical diffusion but including convection, showed no degradation of correlation compared to the reference simulation.

With no convection, mineral aerosol stays near the surface, and near-source removal can take place more efficiently (see also Table 3). Convection appears to be the main process bringing aerosol up to altitudes where it undergoes long-range transport These results emphasize the need for three-dimensional simulations of mineral dust.

5.6. Sensitivity to ECMWF Wind Fields

The good correlation between simulated dust clouds and satellite observation for a sequence of days, at noon over the Mediterranean Sea, indicates that the transport is very well represented in this model. The ECMWF wind fields allow us to mimic well atmospheric transport, and the relatively coarse grid is capable of resolving the evolution of the dust clouds on a timescale of hours. Varying the removal rate of the injected aerosol, either by increasing the mass median diameter and/or the standard deviation of the dust size distribution at the source, did not affect the correlation as long as some aerosol had been transferred to high-altitude layers.

Less accurate wind fields should therefore degrade the result. In simulation O we reduced the frequency with which we read new wind fields to 24 hours Correlation with satellite-derived dust fields decreases slightly. On the basis of variation caused by other parameters this is a significant change. An increase in threshold wind velocity for dust rise will probably enhance the sensitivity to this parameter. In contrast, 12-hourly wind fields are sufficient to reproduce the dust clouds with an accuracy comparable to the reference simulation (not shown).

6. Conclusions

The off-line global 3-D tracer model, based on analyzed wind fields, follows the evolution of the aerosol size distribution. Hence we can retrieve both aerosol number and mass concentration as well as optical thickness Aerosol mass budgets can be computed accounting for gradual changes in size distribution during transport. Furthermore, we have developed a diagnostic tool for the direct comparison of simulated aerosol fields with analyzed satellite observations on a day-by-day and point-by-point basis for any region of interest. The good correlation between simulated fields of dust optical thickness and those derived from satellite gives us confidence that we represent well how atmospheric processes affect the desert dust geographical distribution.

The largest uncertainty in reproducing the position of the dust clouds is linked to the correct localization of the source regions. The agreement with daily changes in dust load over the eastern and western Mediterranean basin shows that we determined the most important source region for the simulation of the Mediterranean dust plume and that the model's coarse resolution (2.5°x2.5°) is sufficient to represent the spatial distribution of dust. Less agreement is found over the Atlantic, especially in regions remote from the African coast. This is due to the lack of sources to the west of our central Saharan source location.

Convection is among the most important atmospheric processes which produce the dust plumes. The transport of dust to higher altitudes by convective updrafts seems to be the prerequisite for the long-range transport to ocean sites. This is supported also by the observation of dust layers over the Mediterranean at 2-4 km height, being correctly simulated by our 3-D model.

The experiments show that when size distributions include a large fraction of coarse particles, unrealistically high dust emissions are necessary to reproduce satellite-derived optical depth. A major aerosol mode having initially a mass median diameter of 2.5 μm and a standard deviation of 2.0 and representing 80% of the total emission flux was found to give a satisfying solution. With this size distribution and the reference provided by satellite optical depth, we have inferred a source strength of 17×10^{12} g for our case study June 25 to July 10, 1988). This source strength agrees well with previous estimates. We would like to emphasize that an aerosol model missing the information on size distribution cannot be constrained by concentration or optical thickness data alone. The sensitivity studies do also demonstrate that the major mode of the mineral aerosol with mmd of 2-3 μm needs to be better documented by measurements of size and column height distribution.

We have shown that the spectral scheme is computationally efficient and accurate for size distributions with a standard deviation of no more than 2.0. A comparable run with 20 bins requires 5 times more computer time on a C90 supercomputer. An accurate numerical treatment of the sedimentation process including a slopes scheme analogy and multilayer crossing in one time step was found to be necessary to minimize numerical diffusion.

The model catches the instantaneous variability of mineral dust concentrations below the daily timescale. This is suggested to provide the proper basis for investigating the effects of extreme events on global budgets of dust transport and radiative effects. Though optical thickness might be better derived from satellite measurements, only a validated model would allow us to make predictions for the future and the past. Model developments under way include the treatment of the wet deposition which will be described in a follow up paper. The incorporation of the Sahara source model as produced by *Marticorena and Bergametti* [1995] will be the basis for multiyear simulations to derive a climatology of mineral dust.

Finally, the inclusion of the treatment of size distribution can also improve our comprehension of the distribution of aerosol components other than mineral dust.

Acknowledgment. We would like to thank Cyril Moulin, Claude Lambert and Frederic Guillard for their tedious work on the satellite raw images. This work would also not have been possible without the model code provided and explained to us by Martin Heimann and its zoom version written by Michel Ramonet. Beatrice Marticorena and Gilles Bergametti provided us both with considerable advice and with source fluxes from their model for a sensitivity run. We are grateful to the CEA for providing generous hospitality and computing facilities. The work of Michael Schulz was partly funded under the EU fellowship programme 'Human Capital and Mobility' (contract ERBCHBGCT 920236). Further support came from the German-French co-operation fund PROCOPE and the EU-ENVIRONMENT and CLIMATE project SINDICATE (contract EV5V-CT92-122). This is CFR contribution No 1990 and LMCE contribution No 413.

References

Andreae, M. O., Raising dust in the greenhouse, *Nature*, *380*, 389-390, 1996.

Bérenger, M., Contribution à l'étude des lithométéores, *La Météorologie*, *72*, 347-374, 1963.

Bergametti, G., Atmospheric cycle of desert dust, in *Encyclopedia of Earth System Science*, pp.171- 182, Academic, vol. 1, San Diego Calif., 1992.

d'Almeida, G. A., A model of Saharan dust transport, *J. Clim Appl. Meteorol.*, *25*, 903-916, 1986.

d'Almeida, G. A., On the variability of aerosol radiative characteristics, *J. Geophys Res.*, *92*, 3017-3026, 1987.

Dentener, F. J., G. R. Carmichael, Y. Zhang, and P Crutzen, P., Role of mineral aerosol as a reactive surface in the global troposphere, *J. Geophys. Res*, *101*, 22869-22889, 1996.

Dulac, G., P. Buat-Ménard, U Ezat, S Melki, and G. Bergametti, Atmospheric input of trace metals to the western mediterranean: Uncertainties in modelling dry deposition from cascade impactor data, *Tellus, Ser B, 41*, 362-378, 1989

Dulac, F., D. Tanré, G. Bergametti, P. Buat-Ménard, M Desbois, and D. Sutton, Assessment of the African airborne dust mass over the western Mediterranean sea using Meteosat data, *J. Geophys Res.*, *97*, 2489-2506, 1992a

Dulac, F., G. Bergametti, R Losno, E. Remoudaki, L. Gomes, U Ezat, and P Buat-Ménard, Dry deposition of mineral aerosol particles in the marine atmosphere: Significance of the large size fraction, in *Precipitation Scavenging and Atmosphere-Surface Exchange*, edited by S.E. Schwartz and W.G.N. Slinn, vol. 2, pp. 841-854, Hemisphere Washigton, D.C., 1992b.

Dulac, F., C. Moulin, C E. Lambert, F. Guillard, J. Poitou, W. Guelle, C. R. Quétel, X. Schneider, and U. Ezat, Quantitative remote sensing of African dust transport to the Mediterranean, in *The Impact of Desert Dust From Northern Africa Across the Mediterranean*, edited by S. Guerzoni and R. Chester, pp. 25-49, Kluwer, Acad., Norwell, Mass.,1996.

Genthon, C., Simulations of desert dust and sea-salt aerosols in Antarctica with a general circulation model of the atmosphere, *Tellus, Ser. B, 44*, 371-389, 1992.

Goudie, A. S., and N. J. Middleton, The changing frequency of dust storms through time, *Clim. Change*, *20*, 197-225, 1992.

Heimann, M., *The global atmospheric tracer model TM2, Tech. Rep 10*, Klimarechenzent., Hamburg, Germany, 1995.

Heimann, M, and C. D. Keeling, A three-dimensional model of atmospheric CO_2 transport based on observed winds, 2, Model description and simulated tracer experiments, in *Aspects of Climate Variability in the Pacific and the Western Americas, Geophys. Monogr. Ser.*, vol *55*, edited by D. H. Peterson, 237-275, AGU, Washington, D.C., 1989.

Houghton J. T., L.G. Meira Filho, J. Bruce, Hoesung Lee, B.A. Callander, E. Haites, N. Harris, and K. Maskel (Eds.), *Climate Change 1994· Radiative Forcing of Climate Change*, Cambridge Univ. Press, Cambridge, *New York*, 1994.

Husar, R B., L. L. Stowe, and J. Prospero, Characterization of tropospheric aerosols over the oceans with the advanced very high resolution radiometer optical thickness operational product, NOAA, *J. Geophys. Res., 102*, 16889-16909, 1997.

Ignatov, A. M., L. L. Stowe, S. M. Sakerin, and G. K. Kozotaev, Validation of the NOAA/NESDIS satellite aerosol product over the North Atlantic in 1989, *J. Geophys. Res., 100, 5123-5132*, 1995.

Jaenicke, R., Aerosol physics and chemistry, in *Landolt-Börnstein Numerical Data and Functional Relationships in Science and Technology*, vol 4b, edited by G. Fischer, pp. 391-457, Springer-Verlag, New York, 1987.

Jankowiak, I., and D. Tanré, Satellite climatology of Saharan outbreaks, *J. Clim., 5*, 646-656, 1992.

Joussaume, S., Three-dimensional simulations of the atmospheric cycle of desert dust particles using a general circulation model, *J. Geophys. Res., 95*, 1909-1941, 1990.

Legrand, M., Etude des Aerosols Sahariens au-dessus de l'Afrique a l'aide du canal a 10 microns de Meteosat: Visualisation, interpretation et modelisation, Thèse de Doctorat, Univer. des Sci. et Tech. de Lille, Lille, France, 1990.

Louis, J.F., A parametric model of vertical eddy fluxes in the atmosphere, *Boundary Layer Meteorl., 17*, 187-202, 1979.

Marticorena, B., Modelisation de al production d'aerosols desertiques en regions arides et semi-arides: Developpement et validation d'un code de calcul adapte au transport a grande echelle, dissertation, Univ. de Paris VII, Paris, 1 995.

Marticorena, B , and G. Bergametti, Modelling the atmospheric dust cycle, 1, Design of a soil-derived dust emission scheme, *J. Geophys. Res., 100*, 16415-16430, 1995.

Martin, J.H., and S.E. Fitzwater, Iron deficiency limits phytoplancton growth in the north-east Pacific subarctic, *Nature, 331*, 341-343, 1988.

Martin, J.H., et al., Testing the iron hypothesis in ecosystems of the equatorial Pacific Ocean, *Nature, 371*, 123-129, 1994.

Middleton, N J., Effect of drought on dust production in the Sahel, *Nature, 316*, 431-434, 1985.

Moulin, C., C E. Lambert, J. Poitou, and F. Dulac, Long-term (1983-1994) calibration of the Meteosat solar (VIS) channel using desert and ocean targets, *Int. J. Remote Sens., 17*, 1183-1200, 1996.

Moulin, C , F. Guillard, F. Dulac, C. E. Lambert, Long-term daily monitoring of Saharan dust load over ocean using Meteosat ISCCP-B2 data, 1, Methodology and preliminary results for 1983-1994 in the Mediterranean, *J. Geophys. Res., 102*, 16947-16958, 1997a.

Moulin, C , F. Dulac, C. E. Lambert, P. Chazette, I Jankowiak, B. Chatenet, and F. Lavenu, Long-term daily monitoring of Saharan dust load over ocean using Meteosat ISCCP-B2 data, 2, Accuracy of the method and validation using Sun photometer measurements, *J Geophys. Res., 102*, 16959-16969, 1997b.

Nickovic, S., and S. Dobrivic, A model for long-range transport of desert dust, *Mon Weather. Rev., 124*, 2537-2544, 1996.

Ramonet, M., Variabilité du CO_2 atmosphèrique en regions Australes: Comparaison modèle/ mesures, Thèse de Doctorat, Univ. de Paris VII, Paris, 1994.

Reiff, J., G S. Forbes, F.T M Spieksma, and J.J. Reynders, African dust reaching northwestern Europe: A case study to verify trejectory calculations, *J. Climate Appl. Meteorol., 25*, 1543-1567, 1986.

Russell, G L., and J. A. Lerner, A new finite-differencing scheme for the tracer transport equation, *J. Appl. Meteorol., 20*, 1483-1498, 1981.

Schütz, L., Long range transport of desert dust with special emphasis on the Sahara, *Ann. N. Y. Acad. Sci., 338*, 515-532, 1980.

Seinfeld J. H., *Air Pollution*, John Wiley, New York, 1986.

Shao, Y., M.R. Raupach, and P.A. Findlater, Effect of saltation bombardment on the entrainment of dust by wind, *J. Geophys. Res., 98*, 12719-12726, 1993.

Shettle, E.P., Optical and radiative properties of a desert aerosol model, *in Proceedings of the Symposium on Radiation in the Atmosphere*, edited by G. Fiocco, pp. 74-77, A. Deepak, Hampton, Va , 1984

Slinn, S.A., and W.G.N. Slinn, Prediction for particle deposition on natural waters, *Atmos. Environ., 14*, 1013-1016, 1980.

Swap, R., M. Garstang, S. Greco, R. Talbot, and P. Källberg, Saharan dust in the Amazon basin, *Tellus, Ser. B, 44*, 133-149, 1992.

Swap, R., S. Ulanski, M. Cobbett, and M. Garstang, Temporal and spatial characteristics of Saharan dust outbreaks, *J. Geophys. Res., 101*, 4205-4220, 1996

Tanré, D., C. Deroo, P. Duhaut, M. Herman, J. J. Morcrette, J. Perbos, and P. Y. Deschamps, Description of a computer code to simulate the satellite signal in the solar spectrum: The 5S code, *Int. J. Remote Sens.*, *2*, 659-668, 1990.

Tegen, I., and I. Fung, Modeling of mineral dust in the atmosphere: Sources, transport, and optical thickness, *J. Geophys. Res.*, *99*, 22897-22914, 1994.

Tegen, I., A.A. Lacis, and I. Fung, The influence on climate forcing of mineral aerosols from disturbed soils, *Nature*, *380*, 419-422, 1996.

Tiedtke, M., A comprehensive mass flux scheme for cumulus parameterization in large-scale models, *Mon. Weather Rev.*, *117*, 1779-1800, 1989.

Westphal, D.L., O. B. Toon, and T. N. Carlson, A case study of mobilization and transport of Saharan dust, *J. Atmos. Sci.*, *45*, 2145-2175, 1988.

Y J. Balkanski and W. Guelle, Laboratoire de Modélisation du Climat et de l'Environnement, CEA, CE Saclay, l'Orme des Merisiers, F-91191 Gif-sur-Yvette Cedex, France. (e-mail: yves.balkanski@cea.fr; guelle@asterix.saclay.cea.fr)

F. Dulac, Centre des Faibles Radioactivités, CNRS-CEA, F-91191 Gif-sur-Yvette Cedex, France. (e-mail: dulac@cea.fr)

M. Schulz, Institut für Anorganische und Angewandte Chemie, Universität Hamburg, Martin-Luther-King-Platz 6, D-20146 Hamburg, Germany. (e-mail: michael.schulz@dkrz.de)

(Received July 10, 1996; revised September 24, 1997; accepted September 24, 1997.)